Self-consistent-field calculation of the structure of the static properties of the solid-fluid interface: The monomer systems

Xiang-Yang Liu
RIM, Laboratory of Solid State Chemistry, Faculty of Science, University of Nijmegen, Toernooiveld, 6525 ED Nijmegen, The Netherlands
(Received 13 July 1993)

A study of the interface between the crystal phase and the fluid phase has been carried out using self-consistent-field theory calculations. The results are expressed in terms of two interfacial factors: the surface characteristic scaling factor C_l^* and the characteristic thickness of the interface n^*. The interfacial structure and interfacial properties can be described employing those two factors. The influence of various parameters, such as the bulk concentration and energy parameters, on the structure and properties of interfaces are discussed in terms of C_l^* and n^*. As a consequence, the surface free energies of some metal systems are estimated from the calculated results. They are compared with experimental values, and turn out to be in good agreement with them. Finally, the interfacial bond energies for some inorganic and metal crystals are analyzed, based on the calculated results in the context of the wetting condition.

PACS number(s): 68.45.Gd, 68.35.Md, 65.50.+m, 68.10.Cr

I. INTRODUCTION

Information on the structure of crystal surfaces can improve our understanding of a number of important physical processes. Crystal growth is one of the processes that take place primarily at the crystal-fluid interface, and hence is strongly influenced by the atomic arrangements in this region. To study the interface of crystals, monomer fluid systems are a good starting point. Many inorganic and metal systems can be treated as monomer systems. In other words, monomer systems represent a large number of real crystal systems. Because these systems are relatively simple, detailed investigations on them have been carried out, using Monte Carlo (MC), molecular-dynamics (MD) computer simulations [1–3] and density-functional theories [4–7]. The results obtained from those methods reveal important information at the interface concerning the ordering of the fluid units in the regions adjacent to the solid surface, surface melting, etc. However, it is not always easy to interpret those results and to associate them with measurable properties (such as the step energy at the surface). Also, MD and MC techniques involve a large number of parameters and sometimes require a large computer capacity.

The same purpose may also be achieved by statistical mechanical calculations based on a self-consistent-field (SCF) theory [8–10], which provides insight into the behavior of structural units in interfacial regions. SCF calculations rely comparatively less on computer capacity than do MD or MC techniques. The quality of the outcome of such calculations depends on how rigorously the partition function is derived. In addition, the results can easily be interpreted within the framework of an inhomogeneous cell model developed recently [11–14].

In the field of crystal growth, the interfacial bond energies ϕ_i are one of the most crucial parameters. The values of ϕ_i at the surfaces $\{hkl\}$ determine the growth mechanism of the surfaces and, e.g., the critical temperature of surface roughening. (The subscript i denotes the interaction between a structural unit and its neighbors in direction i). Due to the inhomogeneity of the interfacial regions, the interfacial bond energy is in most cases different from the bond energy in the bulk [11,12]. In the language of cell models [11], ϕ_i can be expressed for a two-component (A,B) solution system as

$$\phi_i=\tfrac{1}{2}(\phi_i^{AA}-\phi_i^{SS})+[1-X_A(0)]^2\phi_i^{\sigma}+\Delta_i \ , \tag{1}$$

where

$$\phi_i^{\sigma}=\phi_i^{AB}-\tfrac{1}{2}(\phi_i^{AA}+\phi_i^{BB}) \tag{2}$$

and

$$\Delta_i=X_A(0)(\phi_i^{SA}-\phi_i^{AA})+[1-X_A(0)](\phi_i^{SB}-\phi_i^{AB}) \tag{3}$$

(the superscripts AA, BB, SS, AB, SA, and SB represent solute-solute, solvent-solvent, solid-solid, solute-solvent, solid-solute, and solid-solvent interactions, respectively; $X_A(0)$ is the concentration of the solute in the first fluid layer adjacent to the crystal phase.) As an approximation [12], it is assumed that $\phi_i^{SA}\simeq\phi_i^{AA}$ and $\phi_i^{SB}\simeq\phi_i^{AB}$. It then follows that $\Delta_i\simeq 0$.

To associate ϕ_i with the corresponding bond energy in the bulk Φ_i [Φ_i has a form similar to (1), with $\Delta_i=0$], a so-called surface characteristic scaling factor C_l^* is introduced [12]. This factor is defined as

$$C_l^*=\frac{\Delta\tilde{H}_{\rm diss}^{I}}{\Delta\tilde{H}_{\rm diss}}\simeq\frac{\phi_i}{\Phi_i} \ . \tag{4}$$

Here $\Delta\tilde{H}_{\rm diss}^{I}=\sum_{i=1}^{m}\phi_i$ and $\Delta\tilde{H}_{\rm diss}=\sum_{i=1}^{m}\Phi_i$. According to the inhomogeneous cell model [11,12], C_l^* is directly correlated with the concentration in the following way:

$$C_l^*\simeq\ln X_A(0)/\ln X_A \ , \tag{5}$$

where X_A is the concentration of the solute in the bulk. Based on this surface characteristic scaling factor C_l^*, three distinct cases can be recognized for the solid surface [12]: (i) the equivalent wetting [$C_l^*=1$, or $X_A(0)=X_A$]; (ii) the less than equivalent wetting [$C_l^*>1$, or $X_A(0)<X_A$]; (iii) the more than equivalent wetting [$C_l^*<1$, or $X_A(0)>X_A$]. The equivalent wetting case is an artificial reference state, which happens only in some very special situations. Normally, the other two cases occur. The more than equivalent wetting case implies that the solid surface shows an adsorption of solute units. Considering the boundary condition of cell models, $X_A(z)+X_B(z)=1$ [13,14], this equivalently corresponds to a repulsion between the surface and solvent units. In contrast, the less than equivalent wetting case means that the solid surface shows a repulsion to solute units (or an adsorption to solvent units).

To gain sufficient information about the structure of the crystal-fluid interface, in addition to C_l^* another factor, the so-called characteristic thickness of the interface n^*, is introduced [13]. This factor is defined as

$$[X_A(n^*)-X_A]/[X_A(0)-X_A]=e^{-1} \tag{6}$$

at $z=n^*$. (z is the distance away from the solid surface, and normalized by the interplanar spacing d_{hkl} of the crystal phase in the orientation of the surface). Within this framework, profiles of the concentration of solute units at the interface can be described by an exponential law [13] as

$$X_A(z)=X_A[1+D\exp(-z/n^*)] , \tag{7}$$

where

$$D=X_A^{\zeta}-1 \quad \text{and} \quad \zeta=C_l^*-1 . \tag{7a}$$

Obviously, C_l^* and n^* are the two key factors which determine the interfacial structure of monomer systems. The roughening temperature T^r and the surface free energy of faces $\{hkl\}$ may in principle be estimated if these two factors are available [11–14]. We notice that the interfacial structure is commonly determined by the internal structure of crystals and the mother phase. Any change in these regions may in a subtle way affect the morphology of crystals. Therefore the values of C_l^* and n^* are also relevant for the description of the morphology of crystals [15].

To calculate the values of C_l^* and n^* in certain crystallographic orientations $\{hkl\}$, the SCF calculation is an appropriate technique. This technique allows all molecules to be freely distributed throughout the system. In this way, the equilibrium between the interface and the bulk solution is automatically guaranteed. It follows from the calculations that profiles of the density for monomer systems obey the exponential law given by (7). (This result will explicitly be shown in Sec. III.) Then C_l^* and n^* can easily be extracted from the calculated results.

In this study, I use the SCF method to calculate the factors C_l^* and n^* in various conditions for monomer interfacial systems. The paper is arranged as follows. In Sec. II, principles of the SCF calculation are briefly explained. Section III is devoted to the calculations of various monomer systems. An estimate of the surface free energies for some metals is made based on the calculated results. Finally, some discussions are given in Sec. IV.

II. INHOMOGENEOUS CELL MODELS AND SCF CALCULATIONS

Within the framework of cell models, both the solid and the fluid are divided into cells of equal shape and size. Assume that the fluid phase consists of $M+1$ layers of cells parallel to the surface (see Fig. 1). The layer number z is counted from the surface and runs from 0 (the first fluid layer adjacent to the solid surface) to M (in the bulk solution). Every layer has L cells. Each cell has m nearest neighbors, a fraction λ_0 of these are found in the same layer and a fraction λ_1 in each of the adjacent layers. (Explicitly, $\lambda_0+2\lambda_1=1$.)

For a two-component fluid system (A,B), each cell in the fluid phase is considered to be occupied by a molecule (or a monomer) of type i ($i=A$ or B). (This is the so-called full-occupancy constraint.) Within the framework of regular solution theories, different monomers are supposed to have approximately the same volume.

In a mixture near a surface, a concentration gradient for every type of molecule is found due to spatial restrictions and mutual interactions between molecules and between molecules and the surface. Every individual molecule is subjected to a local potential which depends on the distance from the solid surface and on its chemical nature.

In inhomogeneous cell models [12,13], the chemical potential μ_i is expressed for species i as

$$\mu_i=\mu_i^0(z)+kT\ln X_i(z)=\mu_i^0+kT\ln X_i , \tag{8}$$

where $\mu_i^0(z)$ and μ_i^0 denote the standard chemical potential of species i in layer z and in the bulk, and $X_i(z)$ and X_i the concentration of species i (expressed in mole fraction) in layer z and in the bulk, respectively, k is the

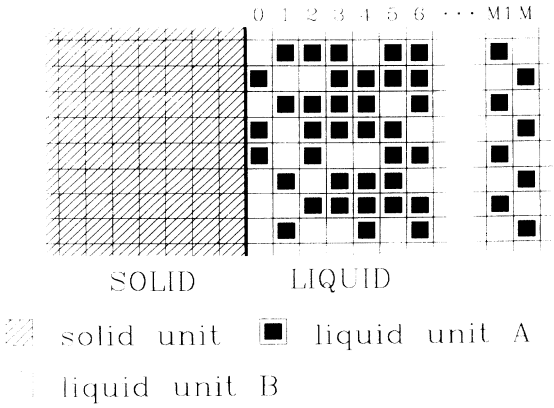

FIG. 1. Illustration of the solid-fluid interface. The fluid phase having M layers of cells parallel to the surface consists of two components A and B. Each cell is filled with either A or B. Cells in the solid phase are only filled with solid units.

Boltzmann constant, and T is the temperature. It then follows that

$$X_i(z)=X_i G_i(z) \tag{9}$$

and

$$G_i(z)=\exp[-u_i(z)/(kT)] \; . \tag{9a}$$

Here $G_i(z)$ is known as the weighting factor [8], and $u_i(z)$ is the (relative chemical) potential and is expressed according to (8) as

$$u_i(z)=\mu_i^0(z)-\mu_i^0 \; . \tag{10}$$

Explicitly, in the bulk phase ($z=M$), $u_i(M)=0$. It can be seen that in case the potential profiles $u_A(z)$, $u_B(z)$,. . . are known, the molecular density (or concentration) profiles $X_A(z)$, $X_B(z)$,. . . can be calculated for every type of molecule. In turn, if the molecular density profiles are known, the potential profiles can be directly calculated.

The SCF theory [8–10] is based on a mean-field approximation within a layer. This implies that fluctuations of the potential within the layer are neglected. From this point of view, the potentials are assumed for solute molecules to be a linear function of the concentrations:

$$u_A(z)=u'(z)+u_A^{\rm int}(z) \tag{11}$$

and

$$u_A^{\rm int}(z)=kT\sum_B \chi_{AB}[\langle X_B(z)\rangle - X_B] \; . \tag{11a}$$

The parameter $u'(z)$ may be interpreted as a "hard-core potential," which guarantees the surface region to be filled by structural units. Actually, it is of both enthalpic and entropic nature. χ_{AB} is the Flory-Huggins interaction parameter, defined as the energy change (in units of kT) associated with the transfer of a molecule of type A from a liquid of pure A into a liquid of pure B. For monomers of equal size, $u'(z)$ is approximately the same for different types of monomers. According to the definition of χ_{AB}, it can be seen that $\chi_{AB}=(1/kT)\sum_{i=1}^{m}\Phi_i^{\sigma}$. [$\Phi_i^{\sigma}$ has an expression analogous to ϕ_i^{σ} in Eq. (2)]. Explicitly, $\chi_{AB}=\chi_{BA}$ and $\chi_{AA}=\chi_{BB}=0$. $\langle X_B(z)\rangle$ is the average concentration of B in layer z, and is given by

$$\langle X_B(z)\rangle=\lambda_1 X_B(z-1)+\lambda_0 X_B(z)+\lambda_1 X_B(z+1) \; . \tag{12}$$

To include the adsorption energy, Eq. (11a) is rewritten for the first fluid layer as

$$u_A^{\rm int}(0)=kT\chi_{AS}\lambda_1+kT\sum_B \chi_{AB}[\langle X_B(0)\rangle - X_B] \; , \tag{11b}$$

where χ_{AS} is the Flory-Huggins parameter for the interaction of an A monomer with surface sites of the adsorbent. For molecules of type B, similar formulas hold. In addition to Eqs. (9)–(12), for the computation in a self-consistent manner, the boundary condition

$$\sum_i X_i(z)=1 \quad \text{for any } z \tag{13}$$

should be fulfilled. This is obviously due to the full occupancy constraint.

To obtain the density (or the concentration) profiles of monomer interfacial systems, the SCF method is to numerically solve the nonlinear equations (9), (9a), (11), and (13). For more details concerning the calculations, see Refs. [8–10].

III. RESULTS

In this section, attention will be focused on two-component systems. According to cell models [12], even for crystals in contact with the melt, the fluid (and the solid) can also be considered as a two-component system. The system consists of structural units and vacuum units. The existence of those vacuum units is due to the free volume in the crystal and the fluid phase. Therefore in interfacial regions the density of structural units changes. Equation (5) can be rewritten in this case as

$$C_l^* \simeq \ln[\rho_f(0)/\rho_s(-1)]/\ln(\rho_f/\rho_s) \; . \tag{5a}$$

(See the Appendix.) Here ρ_f and ρ_s are the densities of the fluid and the solid phase, respectively, $\rho_f(0)$ is the density of fluid units in the first fluid layer adjacent to the solid phase, and $\rho_s(-1)$ is the density of solid units in the first solid layer adjacent to the fluid phase.

A. Influence of macroscopic properties on the interfacial structure

As mentioned in Sec. I, the structure of solid-fluid interfaces can be characterized by two key factors: C_l^* and n^*. On the other hand, once profiles of the density $X_A(z)$ are available, C_l^* and n^* can be easily calculated. Plotting $\ln[X_A-X_A(z)]$ vs z, a linear relation is obtained due to the exponential law expressed by (7) and (7a). Then C_l^* and n^* can be directly calculated from the linear relation. An example of calculated data is shown in Fig. 2.

Note that using the SCF method to calculate $X_A(z)$, some parameters, such as X_A, χ_{AS}, χ_{BS}, and χ_{AB}, are

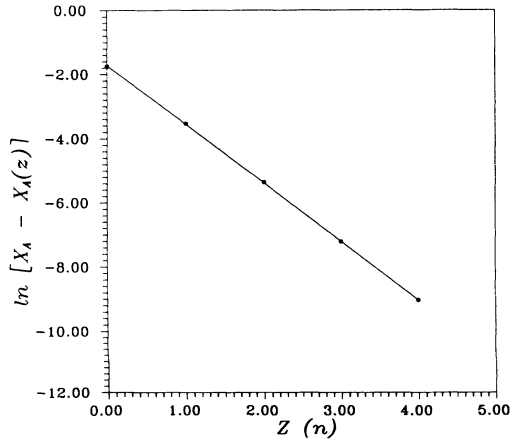

FIG. 2. The linear relation between $\ln[X_A-X_a(z)]$ and the distance z for a monomer system. This relation indicates that the exponential law is valid for monomer systems, $X_A=0.80$, $\chi_{AS}=1.47$, $\chi_{BS}=0$, and $\chi_{AB}=1.47$.

needed. This implies that both C_l^* and n^* are functions of those parameters. Assuming that those parameters are related to bulk properties of interfacial systems, the dependence of C_l^* and n^* on those parameters will be investigated in the following.

Let us first consider the influence of the concentration X_A, under the condition that these energy parameters remain constant. In Fig. 3, C_l^* and n^* are plotted as a function of X_A for systems with $\chi_{AS}=\chi_{AB}=1.47$, $\chi_{BS}=0$. In this case C_l^* remains constant for various concentrations. Only when $X_a \to 1$ does C_l^* decrease slightly [see Fig. 3(a)]. A somewhat different relation can be found between n^* and X_A. It can be seen from Fig. 3(b) that the (characteristic) thickness of the interface decreases almost linearly with X_A. The nonlinearity of the curve occurs when X_A is very close to unity, leading to $n^*=0$. These results indicate that in almost the whole range of X_A (0–1), the thickness of the interface is influenced by the concentration, but C_l^* is not. In case $X_A \to 1$, both C_l^* and n^* have a tendency to approach

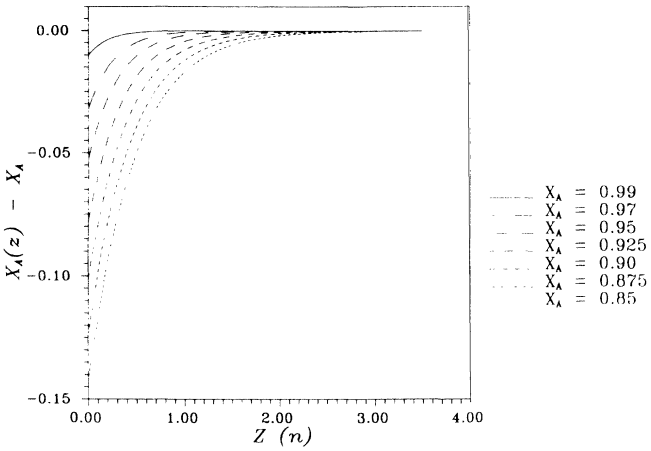

FIG. 4. Profiles of the density $[X_A(z)-X_A]$ plotted vs distance z away from the solid surface for systems with different bulk concentrations.

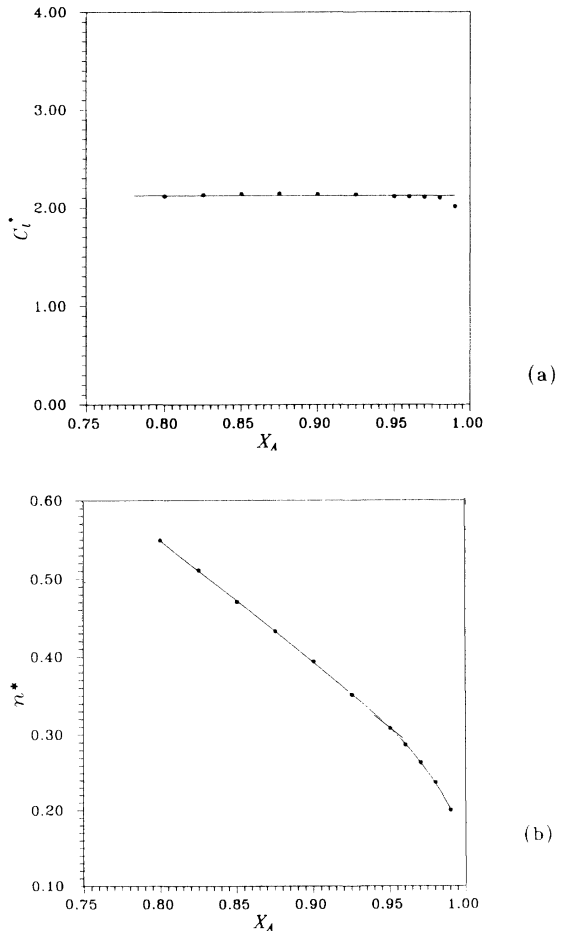

FIG. 3. The relations between the two interfacial factors C_l^* and n^* and the bulk concentration of solute X_A. $\chi_{AS}=\chi_{AB}=1.47$, $\chi_{BS}\simeq 0$. (a) The surface characteristic scaling factor C_l^* plotted vs X_A. C_l^* is almost constant for different concentrations. (b) The characteristic thickness of interfaces n^* plotted vs X_A. n^* linearly decreases with increasing X_A.

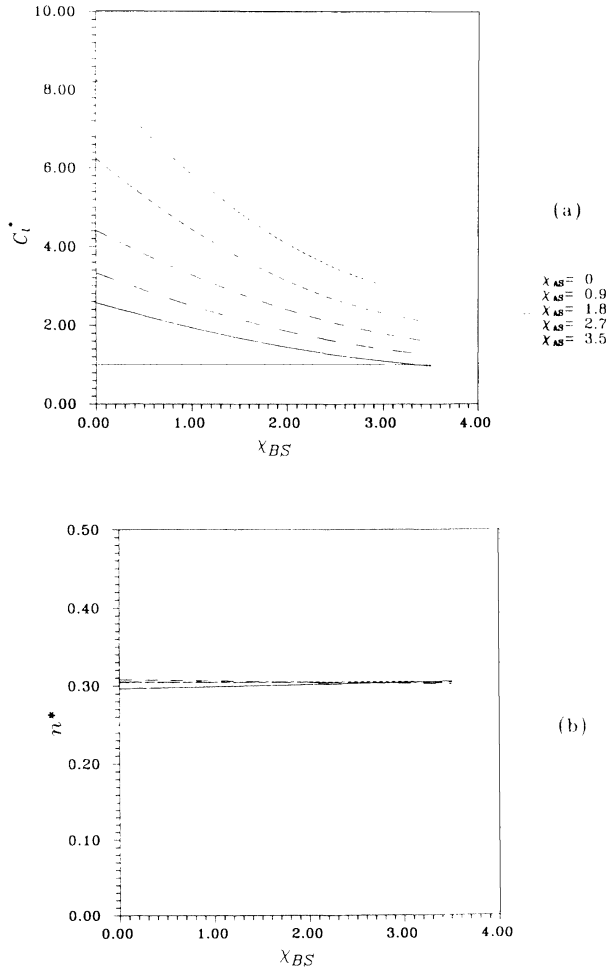

FIG. 5. Dependence of the two interfacial factors n^* and C_l^* on χ_{AS} and χ_{BS} for systems with constant X_A and χ_{AB} ($X_A=0.98$, $\chi_{AB}=3.5$). (a) C_l^* plotted as a function of χ_{BS} (or χ_{AS}). In contrast, C_l^* will increase if χ_{AS} increases. (b) n^* plotted as a function of χ_{BS} (or χ_{AS}). n^* is almost constant for different χ_{AS} and χ_{BS}.

zero, which causes the nonlinearity of the curves. From the point of view of cell models, this particular behavior of C_l^* and n^* at $X_A \to 1$ is understandable. As mentioned earlier, even in the case of crystals in contact with the melt, X_A is smaller than unity ($\simeq \rho_f/\rho_s$). Therefore the fact that $X_A = 1$ implies that differences between the solid and the fluid phase disappear, and the two phases become one phase. It follows that the interface vanishes, resulting in $C_l^* = n^* = 0$. Profiles of the density $[X_A(z) - X_A]$ plotted versus distance z away from the solid surface for systems with various bulk concentrations are given in Fig. 4. This figure, in fact, shows the dependence of the interfacial profiles of the density on n^*.

In contrast to the concentration, the influence of the energy parameters χ_{AS}, χ_{BS}, and χ_{AB} on the interfacial structure are quite complex. It can be seen from Fig. 5 that in case that X_A and χ_{AB} remain constant, varying χ_{AS} or χ_{BS} independently will cause nonlinear changes in C_l^* [see Fig. 5(a)]. n^*, however, remains almost constant [see Fig. 5(b)]. It is shown in Fig. 5(a) that with increasing χ_{BS}, C_l^* is monotonically decreasing. On the other hand, an increase in χ_{AS} will cause an increase in C_l^*. We notice that for most cases discussed in Fig. 5, the less than equivalent wetting occurs ($C_l^* \geq 1$). An increase in χ_{BS} corresponds to a weaker adsorption (or a stronger repulsion) between the solid surface and solvent units. Subsequently, the density of solute in the first fluid layer will become higher. According to (5), this corresponds to the increase of C_l^*. Alternatively, an increase in χ_{AS} corresponds to a weaker adsorption between the solid surface and solute units. In the competition with solvent units, $X_A(0)$ decreases accordingly. This is followed by an increase in C_l^*. In Fig. 6, profiles of the density $[X_A(z) - X_A]$ are plotted versus distance z away from the surface for systems with different χ_{BS}. Differently from Fig. 4, Fig. 6 [combined with Fig. 5(a)] shows the influence on the solid-fluid interfacial structure of monomer systems due to the change of C_l^*.

Keeping X_A constant, simultaneously changing χ_{AS} χ_{BS} and χ_{AB} will cause changes in both C_l^* and n^* (see Fig. 7). For simplicity, assume that $\chi_{AS}:\chi_{BS}:\chi_{AB} = a:b:c$ (a, b, and c are independent constants). Then C_l^* and n^* can be described as a function of χ_{AB}. Obviously, n^* depends linearly on χ_{AB} [Fig.7(a)], while C_l^* turns out to be a nonlinear function of χ_{AB} [Fig. 7(b)]. It is interesting to see that in case the $\chi_{AB} \to \chi'_{AB}$ (curve 1), C_l^* approaches infinity. Referring to Eq. (7), this implies a phase separation. It follows that the solid surface and the solution can probably be separated by pure B layers. In the case of

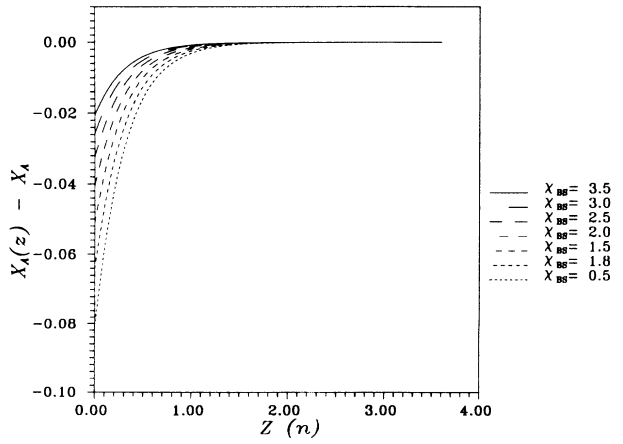

FIG. 6. Profiles of the density $[X_A(z) - X_A]$ plotted vs distance z away from the surface for systems with different χ_{BS}. $X_A = 0.98$, $\chi_{AB} = 3.5$, $\chi_{BS} = 2.7$.

TABLE I. Influence of different crystal structures on the surface scaling factor C_l^* and the characteristic thickness n^*. For this system, $X_A = 0.98$, $\chi_{AS} = 0.267$, $\chi_{BS} = 1.83$, and $\chi_{AB} = 3.50$.

Crystal structure	$\{hkl\}$	$\lambda_1(hkl)$	C_l^*	n^*
FC cubic	{100}	0.333	1.88	0.303
Hexagonal	{001}	0.250	1.63	0.302
BC cubic	{110}	0.250	1.63	0.302
Simple cubic	{100}	0.125	1.40	0.303

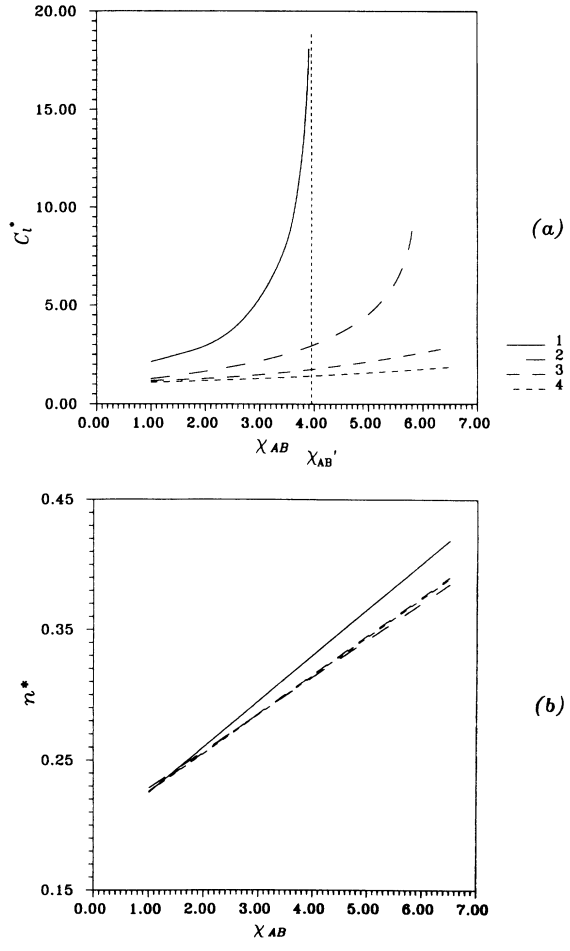

FIG. 7. The influences on C_l^* and n^* due to simultaneously changing χ_{AB}, χ_{AS}, and χ_{BS}. Assume that $\chi_{AS}:\chi_{BS}:\chi_{AB} = a:b:c$. It follows that C_l^* and n^* can be expressed as functions of χ_{AB}. (a) C_l^* vs χ_{AB}; C_l^* depends nonlinearly on χ_{AB}. (b) n^* vs χ_{AB}; n^* is a linear function of χ_{AB}. Curve 1: $a = c = 1$, $b = 0$; Curve 2: $a = b = 0$, $c \neq 0$; Curve 3: $a = 0.076$, $b = 0.52$, and $c = 1$; Curve 4: $a = 0.057$, $b = 0.70$, and $c = 1$.

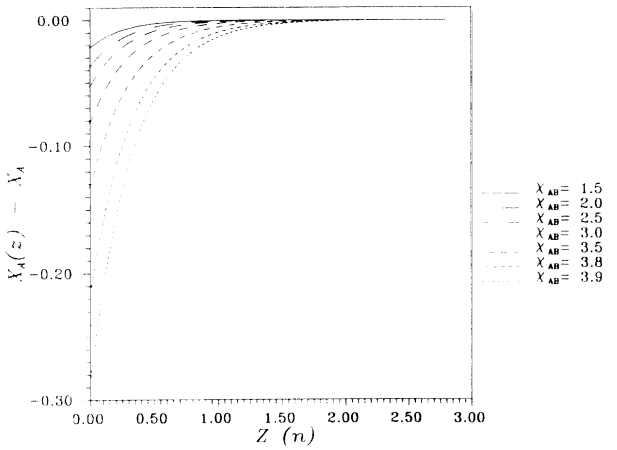

FIG. 8. Profiles of the density $[X_A(z)-X_A]$ plotted vs distance z for systems with different χ_{AB}. $X_A=0.98$, $\chi_{AS}=\chi_{AB}$, $\chi_{BS}=0$.

crystals grown from the melt, gas (or vacuum) is considered as the B component (this corresponds to a larger χ_{AB}). This then implies that bubbles can be easily formed on the solid surface. This has indeed been observed in many crystal-melt systems [16,17].

Note that in Fig. 7, the simple case with $\chi_{AS}=\chi_{BS}=0$, $\chi_{AB}\neq 0$, is shown by curve 2. This case is comparable to the hard-sphere–hard-wall system [1,18]. However, in the system χ_{AB} is a variable which determines the character (or properties) of the systems. In case that surface reconstruction or similar surface phenomena occur, the surface becomes additionally flat, and the interactions between solid and fluid units become relatively weak. This can be seen as an approximation. (We will discuss this in detail in Sec. IV.)

In comparison with Figs. 4 and 6, the influence on the interfacial profiles of the density $[X_A(z)-X_A]$ due to simultaneously changing C_l^* and n^* (via a change in χ_{AB}) are shown in Fig. 8. Because in this case, the two factors C_l^* and n^* change simultaneously, changes in the interfacial structure are more pronounced than in the former two cases.

In spite of those effects mentioned above, the lattice structure also influences C_l^* and n^*. The reason is that different lattice structures have different λ_1 or λ_0. For different structures, C_l^* and n^* are listed in Table I together with λ_1. It can be seen from Table I that a larger λ_1 corresponds to a larger C_l^*. The interpretation can be given as follows. According to the definition of λ_1, the surface excess energy or the adsorption energy of a surface is proportional to λ_1. This implies that the enhancement of λ_1 will lead to an increase in the number of adsorbed solvent units (or B units) in the first fluid layer. (We note that in this case the less that equivalent wetting occurs.) As a result, solute units will decrease in this region [see Eq. (13)], resulting in an increase of C_l^*. λ_1 (or λ_0) is also different for different orientations of the crystal structure. Therefore analogous results can be expected.

B. Estimation of the surface free energy of metals

The concept of surface free energy is relevant for crystal growth. Some important issues in this field are related to its value. However, for most solid-fluid systems, this value is not always available either from experiment or from theory. Therefore it is important if the surface free energy can be estimated.

Conventionally, it is suggested that the surface free energy σ is proportional to the enthalpy of dissolution for a crystal-solution system [19–21] as

$$\sigma s=\xi\Delta\tilde{H}_{\rm diss}\ , \tag{14}$$

where s is the area per surface and ξ a proportionality constant. In case that crystals are in contact with the melt, $\Delta\tilde{H}_{\rm diss}$ should be replaced by the molar enthalpy of melting $\Delta\tilde{H}_m$.

According to our inhomogeneous cell model [14], the coefficient ξ is expressed for crystals in contact with the melt, as

$$\xi\simeq\lambda_1 C_l^*+n^*\frac{\rho_f}{\rho_s}D\left\{-kT_m/\Delta\tilde{H}_m\ln\left[\left[\frac{\rho_f}{\rho_s}\right]\Big/\left[1-\frac{\rho_f}{\rho_s}\right]\right]+\left[\frac{D}{2}\right]\Big/\ln\left[\frac{\rho_f}{\rho_s}\right]\right.$$
$$\left.-\left[\left[\frac{\rho_f}{\rho_s}\right]\frac{D}{2}+\left[\frac{\rho_f}{\rho_s}\right]-1\right]\Big/\left[\left[1-\frac{\rho_f}{\rho_s}\right]\ln\left[1-\frac{\rho_f}{\rho_s}\right]\right]+2\right\}, \tag{15}$$

where T_m is the melting temperature. Note that ρ_f, ρ_s, and $\Delta\tilde{H}_m/T_m$ are bulk properties, and are assumed to be available. If the interfacial factors C_l^* and n^* can be calculated and measured, ξ can be estimated from (15). Then σ may be directly obtained from (14). In this sense, ξ is a key factor to obtain σ.

For metal-melt systems, surface relaxation or surface reconstruction occurs quite often. Therefore accurately estimating the influence of the solid phase on the interfacial fluid structure is difficult. This leads to some difficulties in accurately calculating C_l^* and n^* by the SCF method. (Note that in SCF calculations, the solid phase is to a large extent excluded from direct consideration. Therefore it is implicitly assumed in the calculations that properties of solid units at the surface should not differ too much from those of solid units in the bulk.) However, we can still use simplified models to estimate the values of C_l^* and n^* for metal systems. For this purpose, it is assumed that in a simplified system, $\chi_{AS}=\chi_{BS}=0$ and $\chi_{AB}\neq 0$. This is the case described by

TABLE II. The proportionality constant ξ and some other relevant parameters for three different metal systems.

Metals[a]	$\frac{\Delta\tilde{H}_{ev}}{kT_m}$ [b]	$\frac{kT_m}{\Delta\tilde{H}_m}$ [c]	C_l^*	n^*	ξ Est.	ξ Expt.
Pd	40.0	0.974	3.00	0.314	0.762	0.800[d]
Ag	24.2	0.907	1.87	0.270	0.473	0.457[e]
Cu	27.7	0.868	2.06	0.281	0.520	0.436[e]

[a]Those metals have the fcc structure [19]. Then $\lambda_1=0.25$. $\rho_f/\rho_s\simeq 0.98$ [31].
[b]Reference [32].
[c]Reference [19].
[d]The experimental value of ξ for Pd was determined by Stowell [22].
[e]The experimental values of ξ for Ag and Cu were determined by Turnbull [19].

curve 2 in Fig.7. This corresponds to the system where the fluid is in contact with a very flat and neutral solid surface. In fact, it is a reasonable approximation when the solid surface is very flat due to surface reconstruction or surface relaxation.

In this kind of simplified system, χ_{AB} must be known. As mentioned earlier, in a melt system, fluid units are considered as component A, and vacuum units as component B. Then χ_{AB} is directly related to the evaporation enthalpy $\Delta\tilde{H}_{ev}$ as

$$\chi_{AB}\simeq\nu\Delta\tilde{H}_{ev}/kT_m \ . \tag{16}$$

Here ν is a coefficient. It is found empirically that $\nu\simeq 0.1$. It follows that C_l^* and n^* can be estimated from curve 2 in Figs. 7(a) and 7(b). Consequently, the estimated values of the proportionality constant ξ for three metals Pd, Ag, and Cu are listed in Table II, together with other relevant parameters. In order to make a comparison, the observed values of ξ determined from three-dimensional homogeneous nucleation experiments by Stowell [22] and Turnbull [19] are also listed in this table.

It can be seen from Table II that the estimated values of ξ are in good agreement with the observed values, especially for the value determined by Stowell. In connection with Turnbull's results, there are reports and comments [22–27] indicating that for various reasons, Turnbull's values are a bit too low. (This can also be seen from my estimates.) In this sense, Turnbull's values represent the lowest bound of σ. Considering this fact, my results are quite reasonable.

IV. DISCUSSION AND CONCLUSIONS

It can be seen from the calculated results given in the last section that if solid-fluid interactions at the surface are relatively weak, the so-called less than equivalent wetting case will occur. This has been confirmed by some experimental facts.

According to recent statistical mechanical models [28], a crystal surface undergoes a roughening phase transition at the roughening temperature T^r. If the actual temperature T is lower than the roughening temperature T^r, the surface is flat on a molecular scale. Otherwise, the surface will be rough. The roughening temperature T^r for a given crystal face is directly related to interfacial bond energies ϕ_i, expressed in terms of the dimensionless roughening temperature θ^r, by

$$\theta^r=\frac{2kT^r}{\phi_{str}} \ . \tag{17}$$

Here ϕ_{str} is the strongest bond energy at the surface. Note that θ^r is a dimensionless quantity and has a certain value for a given surface. Obviously, T^r is linearly proportional to ϕ_{str}.

Previously, the roughening temperature has usually been estimated based on the equivalent wetting condition [11,12,28]. This condition implies that in Eq. (17) $\phi_{str}=\Phi_{str}$. However, for many inorganic and metal systems, it turns out that the roughening temperature is underestimated by the equivalent wetting assumption. For instance, Abbaschian and Eslamloo [29] indicated that faceted faces occur on Sn crystals when they grow from the melt. This is in conflict with the obtained estimate that the roughening temperature of the strongest faces on Sn crystals is much lower than the melting point. The growth of garnets from a PbO flux [30] revealed that the bond energies at the (332) faces are almost four times higher than those estimated by the equivalent wetting assumption. Obviously for those systems, $\phi_j>\Phi_j$, meaning that the less than equivalent wetting case occurs.

The presence of the less than equivalent wetting in those systems is to some extent attributed to surface relaxation or surface reconstruction. Because of those surface effects, the interactions between fluid units and the solid surface become weaker. Alternatively, due to the restriction of the solid surface, fluid units will loose some amount of entropy at interfacial regions. The loss of entropy cannot be fully compensated by those very weak solid-fluid interactions at the surface. It then follows that the free energy per fluid unit at the interface will increase, causing a decrease of the density of fluid units at interfacial regions. This finally results in the less than equivalent wetting.

In summary, the dependence of the structure and some thermodynamic properties of monomer interfacial systems on various parameters was studied using SCF theory calculations. As expected, the exponential law can be applied to this kind of system. As an application, the surface free energies of three metal systems were estimated, which turn out to be in good agreement with the experimental results.

ACKNOWLEDGMENTS

Helpful discussions with Dr. F. A. M. Leermakers and Professor Dr. G. J. Fleer are acknowledged. I would like to thank Dr. H. Meekes, Dr. C. S. Strom, and Professor Dr. P. Bennema for a critical reading of this manuscript. I also thank Shell Nederland B. V. for supporting this project.

APPENDIX

According to principles of statistical thermodynamics [12], the chemical potential of structural units is expressed for the fluid and the solid as

$$\mu_f = -kT \ln Q'_f(T) - kT\{\ln v_f + [-\varepsilon_f + (kT)]/(kT)\} \tag{A1}$$

and

$$\mu_s = -kT \ln Q'_s(T) - kT[\ln v_s - \varepsilon_s/(kT)] , \tag{A2}$$

where

$$Q'(T) = [(2\pi m^0 kT)^{3/2}/h^3] Q(T) . \tag{A3}$$

$Q(T)$ denotes the partition function of a molecule for all the internal degrees of freedom, v is the free volume of a molecule, ε is the minimal potential energy per structural unit, m^0 is the mass of a structural unit, h is Planck's constant, and subscripts f and s represent the fluid and the solid phase. At equilibrium, $\mu_f = \mu_s$. It follows that

$$\ln \frac{v_s}{v_f} = -\frac{\Delta \tilde{H}_m}{kT} + \frac{\Delta \tilde{S}'}{k} , \tag{A4}$$

where the melting enthalpy (per structural unit) $\Delta \tilde{H}_m = \varepsilon_f - \varepsilon_s$, and $\Delta \tilde{S}' = k[\ln(Q'_f/Q'_s) + 1]$. Since $\ln(v_s/v_f) \simeq \ln(\rho_f/\rho_s)$, (A4) can be rewritten as

$$\ln(\rho_f/\rho_s) \simeq -\frac{\Delta \tilde{H}_m}{kT} + \frac{\Delta \tilde{S}'}{k} , \tag{A5}$$

where ρ_f and ρ_s denote the density of the fluid and of the solid phase, respectively. If we define $X_A \simeq \rho_f/\rho_s$, then Eq. (A5) assumes an expression similar to the 't Hooft equation. Referring to Eq. (5), X_A can therefore be replaced by ρ_f/ρ_s and $X_A(0)$ by $\rho_f(0)/\rho_s(-1)$. It then follows that Eq. (5) can be rewritten as Eq. (5a).

[1] R. D. Groot, N. M. Faber, and J. P. van der Eerden, Mol. Phys. **60** (1987).
[2] J. Q. Broughton and G. H. Gilmer, J. Chem. Phys. **79**, 5095 (1983); **79**, 5105 (1983); **79**, 5119 (1983); **84**, 5741 (1986); **84**, 5749 (1986); **84**, 5759 (1986).
[3] J. Q. Broughton and F. F. Abraham, Chem. Phys. Lett. **56**, 734 (1986).
[4] T. A. Cherepanova and A. V. Stekolnikov, J. Cryst. Growth **99**, 88 (1990).
[5] A. D. J. Haymet and D. W. Oxtoby, J. Chem. Phys. **74**, 2559 (1981).
[6] M. Baus and J. L. Colot, Mol. Phys. **55**, 653 (1985).
[7] W. A. Curtin and N. W. Ashcroft, Phys. Rev. A **32**, 2909 (1985).
[8] J. M. H. M. Scheutjens and G. J. Fleer, J. Phys. Chem. **83**, 1619 (1979); **84**, 178 (1979).
[9] J. M. H. M. Scheutjens and G. J. Fleer, Macromolecules **18**, 1882 (1985).
[10] F. A. M. Leermakers and J. M. H. M. Scheutjens, J. Chem. Phys. **89**, 3264 (1988); **89**, 6912 (1988); **93**, 7417 (1989).
[11] X. Y. Liu and P. Bennema, J. Chem. Phys. **97**, 3600 (1992).
[12] X. Y. Liu and P. Bennema, J. Chem. Phys. **98**, 5863 (1993).
[13] X. Y. Liu, Surf. Sci. (to be published).
[14] X. Y. Liu, J. Chem. Phys. **98**, 8154 (1993).
[15] X. Y. Liu and P. Bennema, Phys. Rev. E **48**, 2006 (1993).
[16] L. M. Williams, H. Z. Cummins, L. O. Ladeira, and O. N. Mesquita, Phys. Rev. A **45**, 3880 (1992).
[17] J. P. Vesenka and Y. Yeh, J. Cryst. Growth **108**, 19 (1991).
[18] R. D. Groot, Mol. Phys. **60**, 45 (1987).
[19] J. Turnbull, J. Appl. Phys. **21**, 1022 (1950).
[20] M. Kahlweit, Z. Phys. Chem. **28**, 245 (1960).
[21] B. Lewis and J. C. Anderson, *Nucleation and Growth of Thin Films* (Academic, New York, 1970), Chap. 2.
[22] M. J. Stowell, Philos. Mag. **22**, 1 (1970).
[23] D. W. Gomersall, S. Y. Shiraishi, and R. G. Ward, J. Aust. Inst. Metals **10**, 220 (1965).
[24] G. L. F. Powell, J. Aust. Inst. Metals **10**, 223 (1965).
[25] W. A. Miller and G. A. Chadwick, Acta Metall. **15**, 607 (1967).
[26] G. A. Colligan, W. T. Loomis, and V. A. Surprenant, J. Aust. Inst. Metals **10**, 89 (1965).
[27] D. P. Woodruff, *The Solid-Liquid Interface* (Cambridge University Press, London, 1973).
[28] P. Bennema and J. P. van der Eerden, in *Morphology of Crystals*, edited by I. Sunagawa (Terra Scientific, Tokyo, 1987), Part A, p. 1.
[29] G. J. Abbaschian and M. Eslamloo, J. Cryst. Growth **28**, 372 (1975).
[30] W. Tolksdorf and I. Bartels, J. Cryst. Growth **54**, 417 (1981).
[31] *CRC Handbook of Chemistry and Physics*, edited by R. C. Weast (Chemical Rubber, Boca Raton, 1980).
[32] T. Sawada, J. Cryst. Growth **13/14**, 148 (1972).